Biochimica et Biophysica Acta 1828 (2013) 1057–1065

Contents lists available at SciVerse ScienceDirect

Biochimica et Biophysica Acta

journal homepage: www.elsevier.com/locate/bbamem

Does the lipid environment impact the open-state conductance of an engineered β-barrel protein nanopore?

Noriko Tomita [a,b], Mohammad M. Mohammad [a], David J. Niedzwiecki [a], Makoto Ohta [b], Liviu Movileanu [a,c,d,*]

[a] Department of Physics, Syracuse University, Syracuse, NY 13244-1130, USA
[b] Institute of Fluid Science, Tohoku University, Sendai, Miyagi 980-8577, Japan
[c] Structural Biology, Biochemistry, and Biophysics Program, Syracuse University, Syracuse, NY 13244-4100, USA
[d] Syracuse Biomaterials Institute, Syracuse University, Syracuse, NY 13244, USA

ARTICLE INFO

Article history:
Received 6 August 2012
Received in revised form 16 November 2012
Accepted 4 December 2012
Available online 11 December 2012

Keywords:
E. coli FhuA
Planar lipid bilayer
Dimensionless shape factor
Channel closure
Single-channel recording
Lipid effect

ABSTRACT

Using rational membrane protein design, we were recently able to obtain a β-barrel protein nanopore that was robust under an unusually broad range of experimental circumstances. This protein nanopore was based upon the native scaffold of the bacterial ferric hydroxamate uptake component A (FhuA) of *Escherichia coli*. In this work, we expanded the examinations of the open-state current of this engineered protein nanopore, also called FhuA ΔC/Δ4L, employing an array of lipid bilayer systems that contained charged and uncharged as well as conical and cylindrical lipids. Remarkably, systematical single-channel analysis of FhuA ΔC/Δ4L indicated that most of its biophysical features, such as the unitary conductance and the stability of the open-state current, were not altered under the conditions tested in this work. However, electrical recordings at high transmembrane potentials revealed that the presence of conical phospholipids within the bilayer catalyzes the first, stepwise current transition of the FhuA ΔC/Δ4L protein nanopore to a lower-conductance open state. This study reinforces the stability of the open-state current of the engineered FhuA ΔC/Δ4L protein nanopore under various experimental conditions, paving the way for further critical developments in biosensing and molecular biomedical diagnosis.

1. Introduction

Ferric hydroxamate uptake component A (FhuA) is a ligand-gated channel located in the outer membrane (OM) of *Escherichia coli* [1]. This OM protein is a 714-residue monomeric, 22-stranded β-barrel featured by 10 short β-turns on the periplasmic side, 11 long loops on the extracellular side and the 160-residue plug domain within its lumen [2,3] (Fig. 1). The primary function of FhuA is to mediate the energy-driven, high-affinity Fe^{3+} uptake complexed by ferrichrome [4]. In addition, this OM protein serves multiple tasks, including a dual role of transporter and receptor. Its transporter role highlights antibiotic translocation specific for albomycin [5] and rifamycin [6,7], whereas its receptor role is targeted to the colicin M toxin [8] as well as a variety of bacteriophages, including T1, T5 and ϕ80 [9–12]. We presumed that this array of functionalities is a result of a structurally rigid β-barrel scaffold of FhuA [13]. Therefore, we hypothesized that rational membrane protein design characterized by systematic deletion of several extracellular loops and the plug domain will convert a closed OM protein into an open nanopore [14], confirming earlier studies initiated by Braun's and Benz's laboratories [15–18].

Recently, we showed that the removal of four large extracellular loops (4L; L3, L4, L5 and L11) and the plug domain (C), along with a coupling to a fast-dilution protein refolding protocol [19], produced an unusually stable and quiet nanopore, called FhuA ΔC/Δ4L [20,21]. This engineered protein nanopore remained open for long periods under harsh experimental conditions, such as a very acidic pH (3–5) and a broad range of salt concentration in the chamber (between 20 mM and 4 M KCl). The newly created FhuA ΔC/Δ4L protein nanopore represents a deletion of almost one-third of the total number of amino acids of the native FhuA protein (Fig. 1). FhuA ΔC/Δ4L exhibits a conductance of ~4.0 nS in 1 M KCl [20], which is greater than the conductance values observed with other previously studied FhuA deletion mutants [15–18]. Moreover, this engineered nanopore inserts as a monomer in a single orientation into a planar lipid bilayer [20]. These structural and biophysical features imply that FhuA ΔC/Δ4L has potential for applications in

Abbreviations: DPhPC, 1,2-diphytanoyl-*sn*-glycerophosphatidylcholine; DPhPE, 1,2-diphytanoyl-*sn*-glycero-3-phosphoethanolamine; DPhPS, 1,2-diphytanoyl-*sn*-glycero-3-phospho-L-serine; SM, N-palmitoyl-D-erythro-sphingosylphosphorylcholine; ECTPL, *E. coli* total polar lipid extract; FhuA, Ferric hydroxamate uptake component A; FhuA ΔC/Δ4L, Deletion mutant of FhuA lacking the plug domain (C) and four extracellular loops (4L) PE, Phosphatidylethanolamine; PG, Phosphatidylglycerol; CL, Cardiolipin; Bcon, Planar lipid bilayer that includes conically-shaped lipids; Bcyl, Planar lipid bilayer that includes only cylindrically-shaped lipids; FCT, First closure time; NCSS, Normalized current step size; NFCT, Normalized first closure time; VDAC, Voltage-dependent anion channel

* Corresponding author at: Department of Physics, Syracuse University, 201 Physics Building, Syracuse, NY 13244-1130, USA. Tel.: +1 315 443 8078; fax: +1 315 443 9103.
E-mail address: lmovilea@physics.syr.edu (L. Movileanu).

0005-2736/$ – see front matter © 2012 Elsevier B.V. All rights reserved.
http://dx.doi.org/10.1016/j.bbamem.2012.12.003

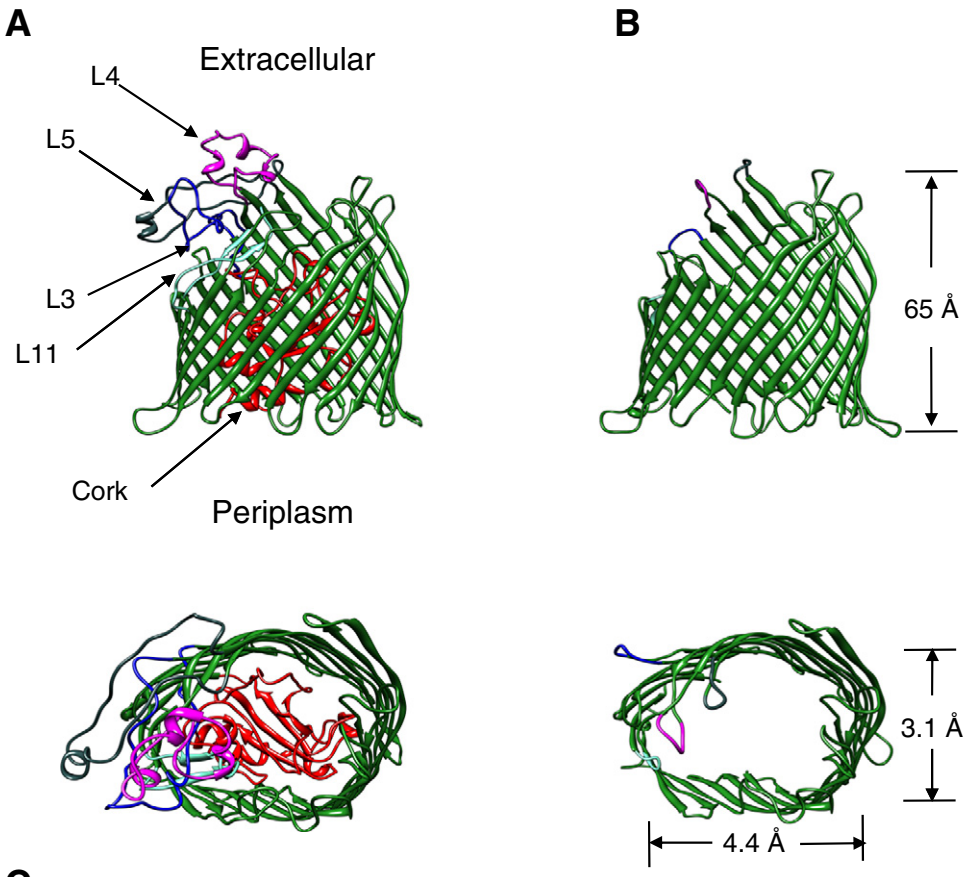

Lipidshape	Inverted cone	Truncated cone	Truncated cone	Cylinder	Cone
Dimensionless shape parameter	<1/3	1/3 –1/2	1/2 - 1	~ 1	> 1
Phase	Spherical micelle	Cylindrical micelle	Lipid vesicle	Planar bilayer	Inverted micelle (Hexagonal (H_{II}))

Fig. 1. The key players in this study: a stiff β-barrel protein nanopore and lipids with various dimensionless shape parameters. The panels indicate the wild-type FhuA (WT-FhuA) (A) and engineered FhuA ΔC/Δ4L proteins (B). The top and bottom panels show the side and extracellular views, respectively. FhuA ΔC/Δ4L protein nanopore was designed by deleting loops L3 (blue), L4 (magenta), L5 (gray), L11 (light green) and the first 160 amino acids (the cork domain, red) of the WT-FhuA protein. These large extracellular loops were replaced with the peptide linkers NSEGS (these linkers have similar color with the deleted loop); (C) A cartoon showing the geometrical shapes of lipids, their corresponding dimensionless shape parameter (*S*) as well as their phase of intermolecular association.

single-molecule stochastic sensing of nucleic acids and proteins [22–27], but also in other biotechnological arenas [28].

We asked whether the electrophysiological characteristics of this stable protein nanopore are impacted by the nature of the lipid environment within the membrane. It is already established that the membrane composition [29], surface tension [30], surface charge [31–34], the nature of polar headgroup [35–38], the degree of acyl chain unsaturation [39], the hydrophobic thickness [37,40,41] and the bilayer curvature [42,43] can play a critical role in promoting the activity, stability, folding, gating and ligand-binding dynamics of the transmembrane proteins. In this

study, we pursued any relationship between the membrane lipid composition and the fundamental properties of the FhuA ΔC/Δ4L protein nanopore. We selected several lipid bilayer systems that included either neutral or negatively charged lipids, but also possessing various dimensionless shape parameters. This work provided new insights into the biophysical features of the engineered FhuA ΔC/Δ4L protein nanopore as well as their dependence on the lipid membrane environment.

2. Materials and methods

2.1. Preparation on planar lipid bilayers

For the preparation of the planar lipid bilayers, we used five types of phospholipids: 1,2-diphytanoyl-*sn*-glycerophosphatidylcholine (DPhPC), 1,2-diphytanoyl-*sn*-glycero-3-phosphoethanolamine (DPhPE), 1,2-diphytanoyl-*sn*-glycero-3-phospho-L-serine (DPhPS), N-palmitoyl-D-erythro-sphingosylphosphorylcholine (SM) and *E. coli* Polar Lipid Extract (ECTPL) containing of phosphatidylethanolamine (PE)/phosphatidylglycerol (PG)/cardiolipin (CL) in a volume ratio of 6.7:2.3:1.0 (Avanti Polar Lipids, Alabaster, AL). Powders of DPhPC, DPhPE, DPhPS and ECTPL were solubilized with pentane at a concentration of 10 mg/ml. The SM powder was solubilized with a mixture of chloroform and methanol in a ratio of 2:1 (v/v). Phospholipid solutions for bilayer formation were prepared by mixing DPhPE and DPhPC in a volume ratio of 3:7 and 1:1, and by mixing SM and DPhPC in a volume ratio of 1:1.

2.2. Preparation of the FhuA ΔC/Δ4L protein

The construction of the plasmid for the protein expression [20,21] as well as the adaptations of the protein refolding protocol for obtaining the engineered FhuA ΔC/Δ4L protein nanopore were described previously [19,20]. Briefly, 40 μL of His^+-tag purified and denatured FhuA ΔC/Δ4L was diluted 50-fold into 1.5% n-Dodecyl-β-d-maltopyranoside (DDM), containing 200 mM NaCl, 50 mM Tris–HCl, 1 mM EDTA, pH 8.0. The diluted protein samples were left overnight at 23 °C for the complete refolding of the FhuA ΔC/Δ4L protein.

2.3. Electrical recordings on planar lipid bilayers

Single-channel electrical recordings were employed using planar lipid bilayers, as published previously [44,45]. The *cis* and *trans* chambers (1.5 ml each) of the apparatus were separated by a 25-μm-thick Teflon septum (Goodfellow Corporation, Malvern, PA). An aperture in the septum, 80–120 μm in diameter, was pretreated with hexadecane (Sigma-Aldrich Co. LLC., St. Louis, MO) dissolved in highly purified pentane (Fisher HPLC grade, Fair Lawn, NJ) at a concentration of 10% (v/v). DPhPE/DPhPC (3:7), DPhPE/DPhPC (1/1), SM/DPhPC (1/1), ECTPL and DPhPS bilayers were formed across the aperture. Single channels of the engineered FhuA ΔC/Δ4L protein were obtained by adding purified and refolded protein to the *cis* chamber at a final concentration of 0.15–0.30 ng/μl. Single-channel electrical recordings were conducted using an Axon 200B patch-clamp amplifier (Axon Instruments, Foster City, CA) in the voltage-clamp mode. Data was collected by an Intel Core Duo PC (Dell, Austin, TX) connected to a Digidata 1440A (Axon Instruments). Output was additionally low-pass filtered at 10 kHz using an 8-pole Bessel filter (Model 900B, Frequency Devices, Ottawa, IL). The acquisition rate was 50 kHz. The data acquisition and analysis were carried out using pClamp 10.2 (Axon Instruments).

2.4. Statistics

The Tukey–Kramer method for multiple comparisons [46,47] was used to compare the unitary conductance values of the engineered FhuA ΔC/Δ4L protein, the normalized current step size (NCSS) values acquired, the number of states, and the normalized first closure times (NFCTs) at an applied transmembrane potential of +180 mV. The Mann–Whitney *U* test [46,47] was also employed to compare the means of the number of states at the applied transmembrane potentials of +40 and +180 mV on each lipid bilayer. The differences were considered significant if $P<0.05$.

3. Results

3.1. Geometrical features of the lipids employed in this work

To examine the effect of various lipids on the single-channel features of the engineered FhuA ΔC/Δ4L protein nanopore, we employed a series of pure and mixed lipid bilayer systems. We used charged and uncharged lipids that are characterized by distinct shapes, such as conical and cylindrical [48]. It is conceivable that the lipid effect strongly depends upon molecular properties, such as hydrocarbon unsaturation, the length of the acyl chain, and the nature of the polar headgroup (e.g., size, ionization etc.). A lipid packing characteristics is determined from the dimensionless shape parameter, *S*, which is given by $S = V/a_0 l_c$, where a_0, l_c and *V* are the optimum area per lipid molecule at the lipid–water interface, the length of the fully extended acyl chain and the molecular volume, respectively [49,50]. The charge and dimensionless shape parameter of all lipid species involved in this work are provided in Table 1.

In Fig. 1C, we illustrate various shapes of phospholipids based upon their dimensionless shape parameter, *S*. For example, phospholipids that have a shape parameter $S \cong 1$ feature a cylindrical geometry, but those with $S<1$ have an inverted or a truncated cone shape [49]. The phospholipids with $S>1$ have the geometry of a cone. To examine the effect of charge, we also employed bilayers with DPhPS, but without being mixed with DPhPC. ECTPL is a mixture of several phospholipids and this was used alone (Table 1). DPhPC is a neutral and cylindrical phospholipid [49,51]. SM is also a neutral and truncated, conical phospholipid [48,52]. On the other hand, PG, CL and DPhPS are cylindrical and negatively charged phospholipids, whereas PE and DPhPE are conical and neutral phospholipids [49–51,53].

The S values in Table 1 are consistent with our observation that DPhPC and DPhPS, whose estimated dimensionless packing parameter, S, is about 1.0, can be employed to form stable lipid bilayers (Supplementary Information, Fig. S1 and Fig. S2). SM, whose estimated S is ~0.51, can also be used to form lipid bilayers, but these are not stable (Supplementary Information, Fig. S3). This observation is likely owing to the truncated conical shape of SM. In general, the SM-containing bilayers break within the first 60 seconds from their original formation. In contrast, mixtures of SM and PC can be employed to form a stable lipid bilayer (Supplementary Information, Fig. S4). DPhPE, whose estimated S is ~1.20, cannot be employed to form a stable lipid bilayer due to its conical shape (Supplementary Information, Fig. S5). However, mixtures of PE and PC can be used to form a stable lipid bilayer (Supplementary Information, Fig. S6 and S7). Finally, we were able to form stable bilayers with ECTPL (Supplementary Information, Fig. S8).

Thus, the overall features of the resultant bilayers inspected in this work led us to divide them into four categories: (i) DPhPE/DPhPC (3:7) and DPhPE/DPhPC (1:1) form neutral bilayers that include conical phospholipids [37], (ii) SM/DPhPC (1:1) forms a neutral bilayer consisting of only cylindrical phospholipids [54], (iii) DPhPS forms a negatively charged bilayer consisting of only cylindrical phospholipids [31], and (iv) *E. coli* total polar lipid extract (ECTPL) forms a negatively charged bilayer that also includes conical phospholipids in the ratio PE/PG/CL (6.7:2.3:1.0) (Avanti) [55]. Those bilayers that include conical phospholipids and those consisting of cylindrical phospholipids are termed Bcon and Bcyl, respectively.

3.2. Single-channel conductance analysis

The single-channel electrical traces were recorded with the engineered FhuA ΔC/Δ4L protein nanopore in 1 M KCl, 10 mM

Table 1
Geometrical properties of the phospholipids employed in this work.

Lipid	Charge	S	a_0 (Å^2)	l_c (Å)	V (Å^3)	References
DPhPC	0	Cylindrical[a] S ~1.00	80.5	13.6	1095	[49,51]
DPhPS	−1	Cylindrical[a] S ~1.06	Unknown Calculated ~79[b]	Unknown 13.6[c]	Unknown 1095[c]	[49,51,53,79]
DPhPE	0	Cone[a] S ~1.20	Unknown Calculated ~67[b]	Unknown 13.6[c]	Unknown 1095[c]	[49,51,53,79]
SM (16:0)	0	Truncated Cone[a] S ~0.51	41[d]	Calculated 21.78[e]	Calculated 457.8[e]	[48,52]
PE (in ECTPL)	0	Cone[f]	~52	Unknown[f]	Unknown[f]	[49,53,80]
PG (in ECTPL)	−1	Cylindrical[f]	~66	Unknown[f]	Unknown[f]	[49,53,80]
CL (in ECTPL)	−2	Cylindrical[f]	Unknown	Unknown[f]	Unknown[f]	[49,80]

[a] The shapes of DPhPC, DPhPS, DPhPE and SM are estimated by a dimensionless shape parameter, S, given by $S = V/a_0 l_c$ [49].
[b] Lipid surface areas of DPhPC and DPhPS are estimated from [51,53], namely, the lipid surface area of diCnPS and diCnPE is 62 Å^2 and 52 Å^2, respectively [51], which are 22% smaller than those of each DPh-form lipids [53]. a_0 (DPhPS) = 62/(1 − 0.22) = 79.4 Å^2, a_0 (DPhPE) = 52/(1 − 0.22) = 66.7 Å^2.
[c] The hydrocarbon lengths and volumes of DPhPS and DPhPC are estimated to be same as DPhPC.
[d] This value is derived from the fully hydrated C16:0 SM at 29 °C.
[e] These values are approximated by the following formula [48]:

$$V \sim (27.4 + 26.9n)\text{Å}^3$$

$$l_c \sim (0.154 + 0.1265n) \times 10\text{Å}$$

[f] l_c and V of PE, PG and CL are unknown, because these are natural lipids extracted from *E. coli*. The shapes of these lipids are referred in [49,80].

potassium phosphate, pH 7.4, and at applied transmembrane potentials between −180 and +180 mV. The single-channel conductance was calculated as the average slope of the standard current–voltage curve. Fig. 2 shows the graphs for the current–voltage (I/V) relationships produced by single FhuA ΔC/Δ4L protein nanopores reconstituted in different lipid bilayer systems. They represent the unitary conductance values of the FhuA ΔC/Δ4L protein nanopore. No statistically significant distinctions were detected among the conductance values of the FhuA ΔC/Δ4L protein nanopore reconstituted in various lipid bilayer systems (Table 2; the Tukey–Kramer method). In general, regardless of the lipid bilayer system employed in this work, we observed that there was an asymmetry in conductance at a positive voltage bias versus a similar negative voltage. For example, in a bilayer with DPhPE/DPhPC (3:7), the average single-channel current was +167 pA at +40 mV, whereas its value was −162 pA at −40 mV.

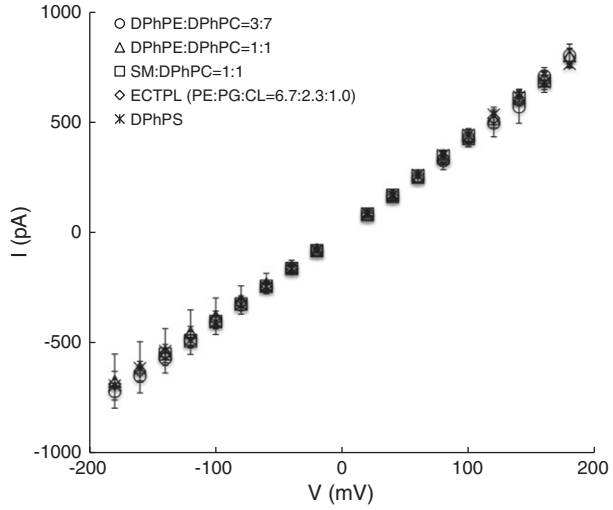

Fig. 2. Single-channel conductance of the engineered FhuA ΔC/Δ4L protein nanopore in different lipid bilayers. Current–voltage (I/V) curves displayed by FhuA ΔC/Δ4L reconstituted into various phospholipid bilayers. The error bars show the standard deviations (SDs) obtained from at least three distinct single-channel recordings. The data were collected in 1 M KCl, 10 mM potassium phosphate, pH 7.4.

3.3. Closing properties of the FhuA ΔC/Δ4L protein reconstituted into various lipid bilayer systems

Fig. 3 illustrates a representative single-channel electrical trace with the FhuA ΔC/Δ4L protein nanopore reconstituted into the DPhPE/DPhPC (3:7) lipid bilayer and at an applied transmembrane potential of +180 mV. At high transmembrane potentials (> 160 mV), the single-channel current decreases in a step-wise fashion owing to the nanopore closure. Recently, we showed that this engineered β-barrel protein inserts into a lipid bilayer in a single orientation and as a monomer [20]. A large-current amplitude closure of an OM protein pore can be caused either by a gating event of one of its monomers, if this is a multimeric protein, or by a discrete conformational alteration of one of the β-barrel loops or turns [56–61]. Therefore, a multi-step decrease in the single-channel current, which was observed with FhuA ΔC/Δ4L at high transmembrane potentials, might be brought about by conformational changes of the extracellular loops or turns of this engineered protein (Fig. 1) [14,59,62–65]. Here, we introduce new parameters that describe the dynamic changes in the single-channel properties of the engineered FhuA ΔC/Δ4L protein reconstituted in different lipid bilayer systems. These are the number of open states, the normalized current step size (NCSS) and the normalized first closure time (NFCT). They are key factors for the assessment of the process of the nanopore

Table 2
Comparison of single-channel conductance of FhuA ΔC/Δ4L reconstituted into various phospholipid bilayers. The buffer solution contained 1 M KCl, 10 mM potassium phosphate, pH 7.4.

Lipid bilayer system	Average single-channel conductance ± SD (nS)
DPhPE:DPhPC = 3:7	4.0 ± 0.5
DPhPE:DPhPC = 1:1	4.1 ± 0.7
ECTPL (PE:PG:CL = 6.7:2.3:1.0)	4.1 ± 0.3
SM:DPhPC = 1:1	4.2 ± 0.4
DPhPS	4.1 ± 0.3

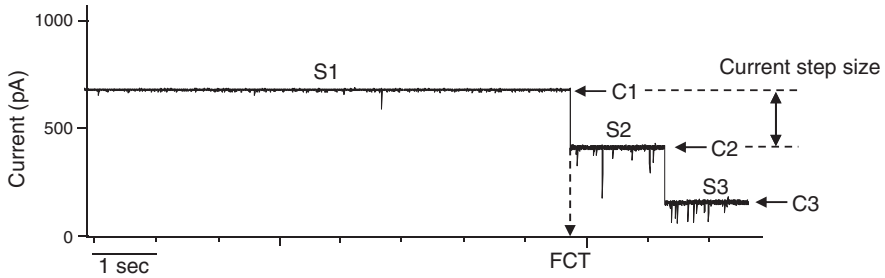

Fig. 3. Representative single-channel electrical recordings of the FhuA ΔC/Δ4L. This single-channel trace is recorded at an applied potential of +180 mV and in 1 M KCl, 10 mM potassium phosphate, pH 7.4. Sn represents the state number of the nanopore at an applied transmembrane potential of +180 mV. S1 is the state of the nanopore before closure. S2 and S3 are the states of a partially closed nanopore. FCT is the first closure time when the nanopore undergoes its first discrete current transition from S1 to S2. The step size denotes the magnitude of the single-channel current decrease by a single closure.

closure, assuming that structural changes of the occluding loops or turns within the protein lumen lead to current alterations.

3.3.1. NCSS and the number of the open states of the channel during the process of closing

The normalized current step size and the number of open states of the FhuA ΔC/Δ4L protein in the process of gradual closing were analyzed using 240-second duration electrical traces at an applied transmembrane potential of +180 mV. As shown in Fig. 3, the open state before closing is termed S1. The following open states are termed Sn (n>1). NCSS used in this study was calculated as the change in the single-channel current from C1 to C2, as compared to the current of the open state C1 (Supplementary Information, Fig. S9):

$$\mathrm{NCSS} = (\mathrm{C1}-\mathrm{C2})/\mathrm{C1} \times 100(\%). \quad (1)$$

Fig. 4 shows the NCSS obtained at the applied transmembrane potential of +180 mV. There is no statistically significant distinction between NCSSs of the protein on the different lipid bilayer systems. At a transmembrane potential of +40 mV, the engineered FhuA ΔCΔ/4L protein nanopore maintained its open-state current for long periods, regardless of the lipid bilayer system examined in this work (Table 3). The number of the open states increased at an applied transmembrane potential of +180 mV. Systematical statistical analysis through the Mann–Whitney *U* test (P<0.05) indicated significant distinctions between the data obtained at +40 mV and +180 mV for each type of lipid bilayer. Using statistical analysis with the Tukey–Kramer method, we did not find significant difference of the NCSSs between any lipid bilayer investigated at an applied transmembrane potential of +180 mV. The NCSS and the number of the states imply intrinsic structural properties that lead to different closure dynamics, resulting in different number of open states of the protein nanopore. These systematical single-channel results indicate that FhuA ΔC/Δ4L forms similar pores on all types of lipid bilayers examined in this work.

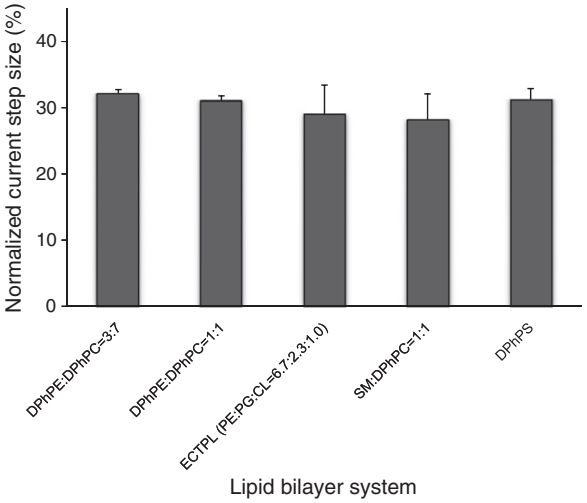

Fig. 4. NCSSs in the process of channel closure of the FhuA ΔC/Δ4L protein reconstituted on various lipid bilayer systems. Each NCSS was calculated according with the Eq. (1). The applied transmembrane potential was +180 mV.

3.3.2. Normalized first closure time (NFCT) of the engineered FhuA ΔC/Δ4L protein nanopore is affected by conical phospholipids

Here, we define the first closure time (FCT) of the protein nanopore as the time taken to undergo its first closure via a discrete step-wise current transition to a second open state. Normalized first closure time (NFCT) is the value of the first closure time normalized to the total duration of the experiment of 60 seconds. If the protein nanopore did not close within 60 seconds, the NFCT was calculated as 1. At least three distinct single-channel experiments were performed for the analysis of NCSS, the number of open states, and NFCT on each kind of lipid bilayer. We did not observe any closing event of the FhuA ΔC/Δ4L protein nanopore at a transmembrane potential of +40 mV. We also investigated the sensitivity of the FhuA ΔC/Δ4L protein for its closure at high transmembrane potentials when reconstituted into lipid bilayers that include cylindrical (Bcyl) and conical phospholipids (Bcon). Fig. 5A shows representative single-channel electrical traces of FhuA ΔC/Δ4L at a transmembrane potential of +180 mV and reconstituted in Bcyl (upper panel) and Bcon (lower panel) bilayers. As shown in Fig. 5B, the NFCTs of the protein nanopore reconstituted on the SM/DPhPC (1:1) and DPhPS bilayers, which are Bcyl, are significantly greater than those data obtained with the DPhPE/DPhPC (3:7), DPhPE/DPhPC (1:1) and ECTPL bilayers, which are Bcon. Taken together, the voltage-induced sensitivity for the very first closure of the nanopore will be impacted by the dimensionless shape parameter of phospholipid constituents of the lipid bilayer system. Moreover, the applied transmembrane potentials determining a first single-channel closure are somewhat lower when conical phospholipids are employed as compared to those values obtained with cylindrical phospholipids. For example, the first single-channel closures with the lipid bilayer systems DPhPE/DPhPC (3:7), DPhPE/DPhPC (1:1) and PS were observed at a transmembrane potential of 80, 100 and 120 mV, respectively (Table 4).

Table 3
Comparison of the number of the open states on various phospholipid bilayers and at applied voltages of +40 mV and +180 mV. The buffer solution contained 1 M KCl, 10 mM potassium phosphate, pH 7.4.

Lipid bilayer system	Average number of open states ± SD	
	+40 mV	+180 mV
DPhPE:DPhPC = 3:7	1	3.3 ± 0.5
DPhPE:DPhPC = 1:1	1	2.8 ± 1.0
ECTPL (PE:PG:CL = 6.7:2.3:1.0)	1	3.3 ± 0.8
SM:DPhPC = 1:1	1	3.7 ± 0.6
DPhPS	1	2.7 ± 0.6

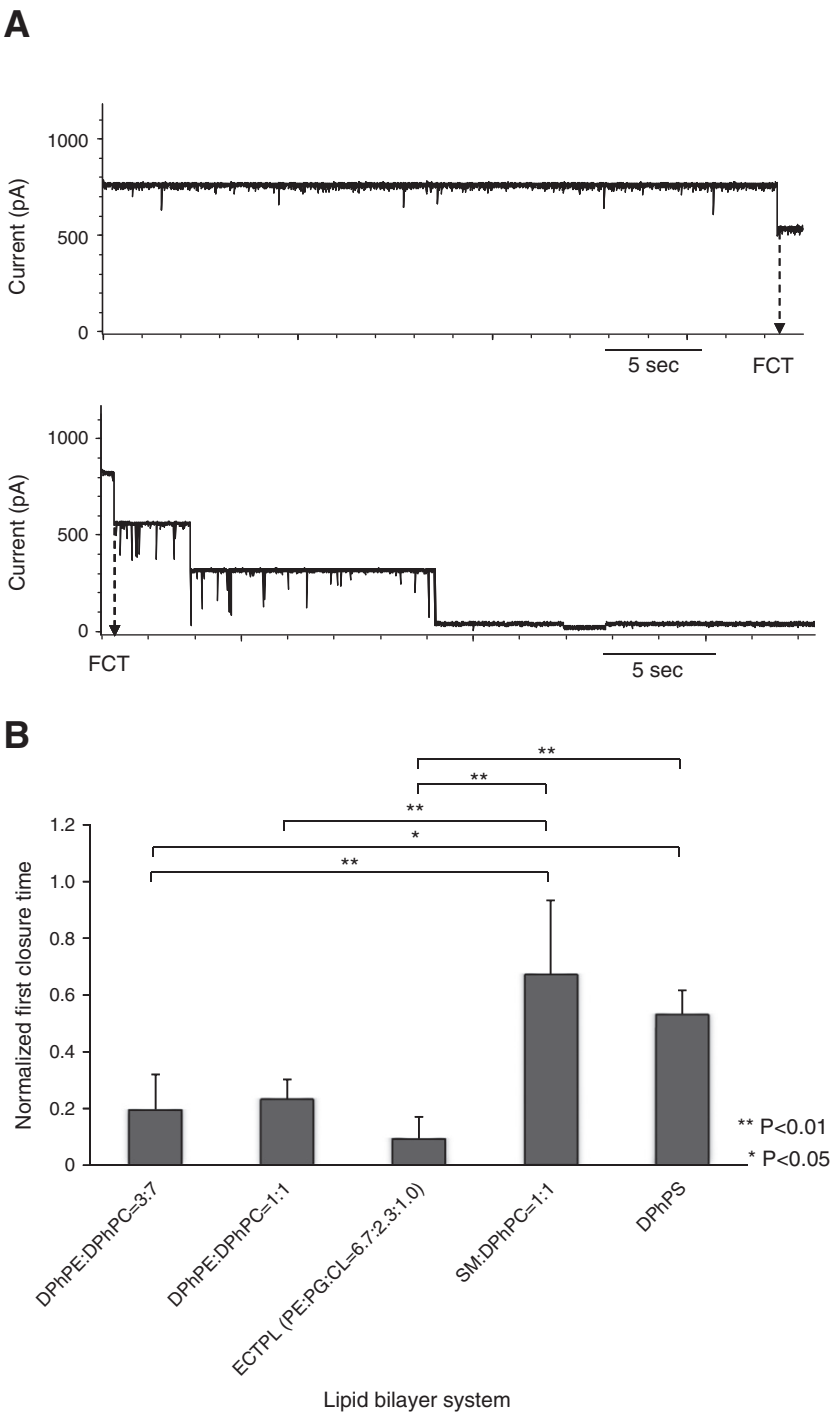

Fig. 5. NFCT of the engineered FhuA ΔC/Δ4L protein nanopore reconstituted into various lipid bilayer systems. (A) Representative examples of single-channel electrical recordings with FhuA ΔC/Δ4L reconstituted into a bilayer formed with either DPhPS (the upper trace) or ECTPL (the lower trace); (B) the NFCTs were analyzed at an applied transmembrane potential of +180 mV. The buffer conditions are the same as in Fig. 2.

4. Discussion

In this work, we performed a systematical single-channel analysis of the engineered FhuA ΔC/Δ4L protein nanopore reconstituted in various lipid bilayer systems. Our primary goal was to examine the alterations in the single-channel features of this β-barrel protein upon its insertion into membranes differing by the nature of constituent lipids. Recently, we determined that coupling of protein engineering with a fast-dilution protein refolding protocol was instrumental in obtaining a rigid β-barrel protein under a broad range of experimental conditions, including pH,

Table 4
Applied transmembrane potentials at which the first single-channel closure of FhuA ΔC/Δ4L is observed.

Lipid bilayer system	Voltage[a] (mV)
DPhPE:DPhPC = 3:7	80
DPhPE:DPhPC = 1:1	100
ECTPL (PE:PG:CL = 6.7:2.3:1.0)	80
SM:DPhPC = 1:1	120
DPhPS	120

[a] Values indicate the positive transmembrane potentials.

applied transmembrane potential and ionic strength in the chamber [20]. Therefore, we asked whether the biophysical properties of this β barrel are impacted by the nature of the lipid environment. Surprisingly, we found that there are no statistically significant modifications of the unitary conductance of FhuA ΔC/Δ4L (~4.1 nS in 1 M KCl, 10 mM potassium phosphate, pH 7.4) when reconstituted in lipid bilayer systems containing either cylindrical or conical phospholipids.

While the FhuA ΔC/Δ4L protein nanopore did not undergo stepwise closure transitions at lower applied transmembrane potentials, it underwent stochastic and stepwise closure transitions to low-conductance open states at greater transmembrane potentials (e.g., +180 mV). We found no statistically significant distinctions in the number of open states and the NCSS when the protein was reconstituted in the bilayer systems examined in this work. However, if the protein was reconstituted into a bilayer containing conical phospholipids, the single-channel electrical traces revealed a faster NFCT than in those bilayers lacking them. By adding conical phospholipids into a Bcyl bilayer, spontaneous curvature stress is produced within the bilayer and lateral pressure is imparted on the embedded membrane protein [42]. We propose that the remaining extracellular loops of the FhuA ΔC/Δ4L affected by the alterations of the packing pressure of bilayer under conditions in which conical phospholipids are present (Fig. 5).

In Fig. 6, we illustrated a model of the free energy landscape of the protein nanopore-lipid bilayer system. This model only shows the open states S1 and S2. The S1 state is the unperturbed high-conductance open state. A thin continuous line represents the free energy associated with a low applied transmembrane potential (e.g., +40 mV), when the protein is embedded into a lipid bilayer containing cylindrical phospholipids. At a high applied transmembrane potential (e.g., +180 mV), the energetic landscape is tilted (thin and dashed curve), showing a smaller activation free energy for a discrete transition to an S2 open state. If the bilayer contains conical phospholipids and the applied potential is low, the transition state corresponding to a stepwise decrease in the single-channel current to a low-conductance S2 open state has a lower energetic level (thick continuous line). Finally, a high applied transmembrane potential coupled with the presence of conical phospholipids into the bilayer produces a decrease of the activation free energy for the current transition from S1 to S2 (thick dashed line).

We judge that the results obtained in this work cannot be generalized to other β-barrel proteins, especially to those exhibiting single-channel current fluctuations. In particular, the OM protein G (OmpG) displays current fluctuations in a neutral DPhPC-based bilayer [66]. Hwang and colleagues (2008) found that the gating kinetics of OmpG is strongly dependent on the charged state of the individual leaflets of the bilayer [38]. For example, when OmpG was inserted from the negative side of the bilayer, the frequency of gating current fluctuations increased as compared to that value obtained with a neutral bilayer. In contrast, the frequency of gating decreased relative to the neutral bilayer, if the protein was inserted from the positive side of the bilayer. A much less intuitive result was obtained by Ishii and Nakae (1993), who examined the OccD1 protein channel of *Pseudomonas aeruginosa*, which is a monomeric, outer membrane β-barrel protein [67]. This protein channel exhibits a unitary conductance of ~30 pS in 1 M KCl DPhPC-based bilayers [60,67–70]. However, Ishii and Nakae discovered frequent large-conductance current openings (~400 pS in 1 M KCl) in bilayers that contained lipopolysaccharides (LPS). Stochastic current transitions in β-barrel proteins might have physiological relevance, especially in the case of substrate-specific small porins of *P. aeruginosa*, requiring further biophysical [36,70–73] and computational examination [74–78].

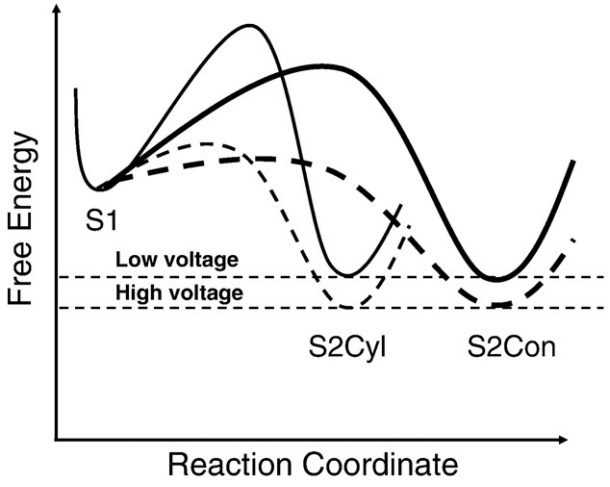

Fig. 6. Schematic model of the free energy landscape of the S1–S2 transitions of the FhuA ΔC/Δ4L–bilayer system. Continue and dashed lines denote the free energy landscape at the applied transmembrane potential of 40 and 180 mV, respectively. Thin and thick lines indicate the data for the Bcyl and Bcon bilayers, respectively. The two horizontal dashed lines show the energetic minima of the S2 state at low (40 mV) and high (180 mV) positive voltages.

Anthony Lee (2004) emphasized that the features of the polar headgroup, such as its structure, size and charge, as well as the characteristics of the hydrogen bonding potential, strongly impact the regions of the transmembrane proteins at the lipid–aqueous phase interface [41]. In addition, phosphatidylethanolamine-based lipids, such as PE and DPhPE, display a susceptibility to form a curved, hexagonal H_{II} phase [49]. Indeed, we confirmed that we were not able to form stable lipid bilayers with PE or DPhPE (Supplementary Information, Fig. S5). However, we accomplished single-channel measurements with the engineered FhuA ΔC/Δ4L protein nanopore reconstituted in lipid bilayers that included mixtures of DPhPE and DPhPC. Importantly, most of the properties of the nanopore remained unaltered in PE-containing lipid bilayer mixtures, such as the unitary conductance, and the current amplitude of the step-size closures and the average number of closing steps at high applied transmembrane potentials. It is conceivable that the conical geometry of PE and the conformation of the polar headgroup have a great effect on the lipid–protein nanopore interactions at the lipid–aqueous phase interface. Such impact was consistently observed with the short duration of the very first step-wise current closure of the FhuA ΔC/Δ4L protein nanopore at a high applied transmembrane potential when data was recorded with PE-containing lipid bilayers. Our results are also consistent with prior findings of Rostovtseva and colleagues (2006), who revealed that the voltage gating of the voltage-dependent anion channel (VDAC) is regulated by the presence of nonlamellar lipids in the membrane [36]. In particular, PE has a major effect on the voltage asymmetry in the current–voltage features and current gating of VDAC.

In summary, we determined that the opening of the FhuA ΔC/Δ4L protein nanopore reconstituted into the cylindrical phospholipid-containing bilayers is maintained for a longer duration compared with those situations employing the conical phospholipid-containing bilayers at high applied transmembrane potentials. Our data indicate that the NCSS and the number of open states of the FhuA ΔC/Δ4L protein nanopore were similar. Taken together, these findings suggest that the shape of the phospholipid can alter the stability of the open-state current of the engineered FhuA ΔC/Δ4L protein nanopore.

Acknowledgements

The authors thank Jiaming Liu and Belete R. Cheneke for technical assistance and stimulating discussions. This work was partly supported by Young Researcher Overseas Visits Program for Vitalizing Brain Circulation (IFS, JSPS) and by a Global COE Program Grant of the World Center of Education and Research for Trans-disciplinary Flow Dynamics from Tohoku University. We also acknowledge support by grants from the US National Science Foundation (DMR-1006332, L.M.) and the National Institutes of Health (R01 GM088403, L.M.). N. Tomita is a recipient of a postdoctoral fellowship from Japan Society for the Promotion of Science.

Appendix A. Supplementary data

Supplementary data to this article can be found online at http://dx.doi.org/10.1016/j.bbamem.2012.12.003.

References

[1] V. Braun, M. Braun, Iron transport and signaling in *Escherichia coli*, FEBS Lett. 529 (2002) 78–85.
[2] K.P. Locher, B. Rees, R. Koebnik, A. Mitschler, L. Moulinier, J.P. Rosenbusch, D. Moras, Transmembrane signaling across the ligand-gated FhuA receptor: crystal structures of free and ferrichrome-bound states reveal allosteric changes, Cell 95 (1998) 771–778.
[3] A.D. Ferguson, E. Hofmann, J.W. Coulton, K. Diederichs, W. Welte, Siderophore-mediated iron transport: crystal structure of FhuA with bound lipopolysaccharide, Science 282 (1998) 2215–2220.
[4] P.D. Pawelek, N. Croteau, C. Ng-Thow-Hing, C.M. Khursigara, N. Moiseeva, M. Allaire, J.W. Coulton, Structure of TonB in complex with FhuA, *E. coli* outer membrane receptor, Science 312 (2006) 1399–1402.
[5] A.D. Ferguson, V. Braun, H.P. Fiedler, J.W. Coulton, K. Diederichs, W. Welte, Crystal structure of the antibiotic albomycin in complex with the outer membrane transporter FhuA, Protein Sci. 9 (2000) 956–963.
[6] M. Braun, H. Killmann, V. Braun, The beta-barrel domain of FhuADelta5-160 is sufficient for TonB-dependent FhuA activities of *Escherichia coli*, Mol. Microbiol. 33 (1999) 1037–1049.
[7] A.D. Ferguson, J. Kodding, G. Walker, C. Bos, J.W. Coulton, K. Diederichs, V. Braun, W. Welte, Active transport of an antibiotic rifamycin derivative by the outer-membrane protein FhuA, Structure 9 (2001) 707–716.
[8] Z. Cao, P.E. Klebba, Mechanisms of colicin binding and transport through outer membrane porins, Biochimie 84 (2002) 399–412.
[9] M. Bonhivers, A. Ghazi, P. Boulanger, L. Letellier, FhuA, a transporter of the *Escherichia coli* outer membrane, is converted into a channel upon binding of bacteriophage T5, EMBO J. 15 (1996) 1850–1856.
[10] L. Letellier, K.P. Locher, L. Plancon, J.P. Rosenbusch, Modeling ligand-gated receptor activity. FhuA-mediated ferrichrome efflux from lipid vesicles triggered by phage T5, J. Biol. Chem. 272 (1997) 1448–1451.
[11] T. Mdzinarashvili, M. Khvedelidze, A. Ivanova, G. Mrevlishvili, M. Kutateladze, N. Balarjishvili, H. Celia, F. Pattus, Biophysics of T5, IRA phages, *Escherichia coli* outer membrane protein FhuA and T5-FhuA interaction, Eur. Biophys. J. 35 (2006) 231–238.
[12] A. Leforestier, S. Brasiles, F.M. de, E. Raspaud, L. Letellier, P. Tavares, F. Livolant, Bacteriophage T5 DNA ejection under pressure, J. Mol. Biol. 384 (2008) 730–739.
[13] M. Bonhivers, M. Desmadril, G.S. Moeck, P. Boulanger, A. Colomer-Pallas, L. Letellier, Stability studies of FhuA, a two-domain outer membrane protein from *Escherichia coli*, Biochemistry 40 (2001) 2606–2613.
[14] M.M. Mohammad, K.R. Howard, L. Movileanu, Redesign of a plugged beta-barrel membrane protein, J. Biol. Chem. 286 (2011) 8000–8013.
[15] M. Braun, H. Killmann, E. Maier, R. Benz, V. Braun, Diffusion through channel derivatives of the *Escherichia coli* FhuA transport protein, Eur. J. Biochem. 269 (2002) 4948–4959.
[16] V. Braun, H. Killmann, R. Benz, Energy-coupled transport through the outer membrane of *Escherichia coli* small deletions in the gating loop convert the FhuA transport protein into a diffusion channel, FEBS Lett. 346 (1994) 59–64.
[17] H. Killmann, R. Benz, V. Braun, Properties of the FhuA channel in the *Escherichia coli* outer membrane after deletion of FhuA portions within and outside the predicted gating loop, J. Bacteriol. 178 (1996) 6913–6920.
[18] H. Killmann, R. Benz, V. Braun, Conversion of the FhuA transport protein into a diffusion channel through the outer membrane of *Escherichia coli*, EMBO J. 12 (1993) 3007–3016.
[19] A. Arora, D. Rinehart, G. Szabo, L.K. Tamm, Refolded outer membrane protein A of *Escherichia coli* forms ion channels with two conductance states in planar lipid bilayers, J. Biol. Chem. 275 (2000) 1594–1600.
[20] M.M. Mohammad, R. Iyer, K.R. Howard, M.P. McPike, P.N. Borer, L. Movileanu, Engineering a rigid protein tunnel for biomolecular detection, J. Am. Chem. Soc. 134 (2012) 9521–9531.
[21] D.J. Niedzwiecki, M.M. Mohammad, L. Movileanu, Inspection of the Engineered FhuA deltaC/delta4L Protein Nanopore by Polymer Exclusion, Biophys. J. 103 (2012) 2115–2124.
[22] D. Branton, D.W. Deamer, A. Marziali, H. Bayley, S.A. Benner, T. Butler, M. Di Ventra, S. Garaj, A. Hibbs, X. Huang, S.B. Jovanovich, P.S. Krstic, S. Lindsay, X.S. Ling, C.H. Mastrangelo, A. Meller, J.S. Oliver, Y.V. Pershin, J.M. Ramsey, R. Riehn, G.V. Soni, V. Tabard-Cossa, M. Wanunu, M. Wiggin, J.A. Schloss, The potential and challenges of nanopore sequencing, Nat. Biotechnol. 26 (2008) 1146–1153.
[23] L. Movileanu, Squeezing a single polypeptide through a nanopore, Soft Matter 4 (2008) 925–931.
[24] S. Howorka, Z. Siwy, Nanopore analytics: sensing of single molecules, Chem. Soc. Rev. 38 (2009) 2360–2384.
[25] L. Movileanu, Interrogating single proteins through nanopores: challenges and opportunities, Trends Biotechnol. 27 (2009) 333–341.
[26] S. Majd, E.C. Yusko, Y.N. Billeh, M.X. Macrae, J. Yang, M. Mayer, Applications of biological pores in nanomedicine, sensing, and nanoelectronics, Curr. Opin. Biotechnol. 21 (2010) 439–476.
[27] S. Howorka, Z.S. Siwy, Nanopores as protein sensors, Nat. Biotechnol. 30 (2012) 506–507.
[28] S. Banta, Z. Megeed, M. Casali, K. Rege, M.L. Yarmush, Engineering protein and peptide building blocks for nanotechnology, J. Nanosci. Nanotechnol. 7 (2007) 387–401.
[29] R. Phillips, T. Ursell, P. Wiggins, P. Sens, Emerging roles for lipids in shaping membrane-protein function, Nature 459 (2009) 379–385.
[30] R. Chiriac, T. Luchian, Single-molecule investigation of the influence played by lipid rafts on ion transport and dynamic features of the pore-forming alamethicin oligomer, J. Membr. Biol. 224 (2008) 45–54.
[31] T.K. Rostovtseva, V.M. Aguilella, I. Vodyanoy, S.M. Bezrukov, V.A. Parsegian, Membrane surface-charge titration probed by gramicidin A channel conductance, Biophys. J. 75 (1998) 1783–1792.
[32] S.J. Alvis, I.M. Williamson, J.M. East, A.G. Lee, Interactions of anionic phospholipids and phosphatidylethanolamine with the potassium channel KcsA, Biophys. J. 85 (2003) 3828–3838.
[33] T.K. Rostovtseva, H.I. Petrache, N. Kazemi, E. Hassanzadeh, S.M. Bezrukov, Interfacial polar interactions affect gramicidin channel kinetics, Biophys. J. 94 (2008) L23–L25.
[34] P.A. Gurnev, M. Queralt-Martin, V.M. Aguilella, T.K. Rostovtseva, S.M. Bezrukov, Probing tubulin-blocked state of VDAC by varying membrane surface charge, Biophys. J. 102 (2012) 2070–2076.
[35] L.K. Tamm, H. Hong, B. Liang, Folding and assembly of beta-barrel membrane proteins, Biochim. Biophys. Acta 1666 (2004) 250–263.
[36] T.K. Rostovtseva, N. Kazemi, M. Weinrich, S.M. Bezrukov, Voltage gating of VDAC is regulated by nonlamellar lipids of mitochondrial membranes, J. Biol. Chem. 281 (2006) 37496–37506.
[37] R.J. O'Connell, C. Yuan, L.J. Johnston, O. Rinco, I. Probodh, S.N. Treistman, Gating and conductance changes in BK(Ca) channels in bilayers are reciprocal, J. Membr. Biol. 213 (2006) 143–153.
[38] W.L. Hwang, M. Chen, B. Cronin, M.A. Holden, H. Bayley, Asymmetric droplet interface bilayers, J. Am. Chem. Soc. 130 (2008) 5878–5879.
[39] L. Mereuta, T. Luchian, Y. Park, K.S. Hahm, The role played by lipids unsaturation upon the membrane interaction of the *Helicobacter pylori* HP(2–20) antimicrobial peptide analogue HPA3, J. Bioenerg. Biomembr. 41 (2009) 79–84.
[40] A.M. Powl, J.M. East, A.G. Lee, Lipid–protein interactions studied by introduction of a tryptophan residue: the mechanosensitive channel MscL, Biochemistry 42 (2003) 14306–14317.
[41] A.G. Lee, How lipids affect the activities of integral membrane proteins, Biochim. Biophys. Acta 1666 (2004) 62–87.
[42] S.M. Gruner, Intrinsic curvature hypothesis for biomembrane lipid composition: a role for nonbilayer lipids, Proc. Natl. Acad. Sci. U. S. A. 82 (1985) 3665–3669.
[43] T. Baumgart, B.R. Capraro, C. Zhu, S.L. Das, Thermodynamics and mechanics of membrane curvature generation and sensing by proteins and lipids, Annu. Rev. Phys. Chem. 62 (2011) 483–506.
[44] M.M. Mohammad, S. Prakash, A. Matouschek, L. Movileanu, Controlling a single protein in a nanopore through electrostatic traps, J. Am. Chem. Soc. 130 (2008) 4081–4088.
[45] M.M. Mohammad, L. Movileanu, Excursion of a single polypeptide into a protein pore: simple physics, but complicated biology, Eur. Biophys. J. 37 (2008) 913–925.
[46] H. Motulsky, Intuitive Biostatistics, Oxford University Press, New York, 1995.
[47] G.P. Quinn, M.J. Keough, Experimental Design and Data Analysis for Biologists, Cambridge University Press, Cambridge, UK, 2002.
[48] J.N. Israelachvili, Intermolecular and Surface Forces, Elsevier Science B.V., Amsterdam 2011, (New York).
[49] P.R. Cullis, M.J. Hope, C.P. Tilcock, Lipid polymorphism and the roles of lipids in membranes, Chem. Phys. Lipids 40 (1986) 127–144.
[50] I. van Uitert, S. Le Gac, A. van den Berg, The influence of different membrane components on the electrical stability of bilayer lipid membranes, Biochim. Biophys. Acta 1798 (2010) 21–31.
[51] S. Tristram-Nagle, D.J. Kim, N. Akhunzada, N. Kucerka, J.C. Mathai, J. Katsaras, M. Zeidel, J.F. Nagle, Structure and water permeability of fully hydrated diphytanoylPC, Chem. Phys. Lipids 163 (2010) 630–637.
[52] P.R. Maulik, G.G. Shipley, N-palmitoyl sphingomyelin bilayers: structure and interactions with cholesterol and dipalmitoylphosphatidylcholine, Biochemistry 35 (1996) 8025–8034.
[53] J.H. Kleinschmidt, L.K. Tamm, Structural transitions in short-chain lipid assemblies studied by (31)P-NMR spectroscopy, Biophys. J. 83 (2002) 994–1003.
[54] T. Ide, T. Aoki, Y. Takeuchi, T. Yanagida, Lysenin forms a voltage-dependent channel in artificial lipid bilayer membranes, Biochem. Biophys. Res. Commun. 346 (2006) 288–292.
[55] E.R. O'Neill, M.M. Sakowska, D.R. Laver, Regulation of the calcium release channel from skeletal muscle by suramin and the disulfonated stilbene derivatives DIDS, DBDS, and DNDS, Biophys. J. 84 (2003) 1674–1689.
[56] P.S. Phale, T. Schirmer, A. Prilipov, K.L. Lou, A. Hardmeyer, J.P. Rosenbusch, Voltage gating of *Escherichia coli* porin channels: role of the constriction loop, Proc. Natl. Acad. Sci. U. S. A. 94 (1997) 6741–6745.
[57] G. Bainbridge, I. Gokce, J.H. Lakey, Voltage gating is a fundamental feature of porin and toxin beta-barrel membrane channels, FEBS Lett. 431 (1998) 305–308.
[58] G. Bainbridge, H. Mobasheri, G.A. Armstrong, E.J.A. Lea, J.H. Lakey, Voltage-gating of *Escherichia coli* porin: A cystine-scanning mutagenesis study of loop 3, J. Mol. Biol. 275 (1998) 171–176.
[59] A. Basle, R. Iyer, A.H. Delcour, Subconductance states in OmpF gating, Biochim. Biophys. Acta 1664 (2004) 100–107.
[60] S. Biswas, M.M. Mohammad, D.R. Patel, L. Movileanu, B. van den Berg, Structural insight into OprD substrate specificity, Nat. Struct. Mol. Biol. 14 (2007) 1108–1109.
[61] S. Biswas, M.M. Mohammad, L. Movileanu, B. van den Berg, Crystal structure of the outer membrane protein OpdK from *Pseudomonas aeruginosa*, Structure 16 (2008) 1027–1035.
[62] H. Samartzidou, A.H. Delcour, E.coli PhoE porin has an opposite voltage-dependence to the homologous OmpF, EMBO J. 17 (1998) 93–100.
[63] Y. Jung, H. Bayley, L. Movileanu, Temperature-responsive protein pores, J. Am. Chem. Soc. 128 (2006) 15332–15340.

[64] C. Chimerel, L. Movileanu, S. Pezeshki, M. Winterhalter, U. Kleinekathofer, Transport at the nanoscale: temperature dependence of ion conductance, Eur. Biophys. J. 38 (2008) 121–125.
[65] M.M. Mohammad, L. Movileanu, Impact of distant charge reversals within a robust beta-barrel protein pore, J. Phys. Chem. B 114 (2010) 8750–8759.
[66] S. Conlan, Y. Zhang, S. Cheley, H. Bayley, Biochemical and biophysical characterization of OmpG: a monomeric porin, Biochemistry 39 (2000) 11845–11854.
[67] J. Ishii, T. Nakae, Lipopolysaccharide promoted opening of the porin channel, FEBS Lett. 320 (1993) 251–255.
[68] J. Ishii, T. Nakae, Specific interaction of the protein-D2 porin of *Pseudomonas aeruginosa* with antibiotics, FEMS Microbiol. Lett. 136 (1996) 85–90.
[69] E. Eren, J. Vijayaraghavan, J. Liu, B.R. Cheneke, D.S. Touw, B.W. Lepore, M. Indic, L. Movileanu, B. van den Berg, Substrate specificity within a family of outer membrane carboxylate channels, PLoS Biol. 10 (2012) e1001242.
[70] J. Liu, A.J. Wolfe, E. Eren, J. Vijayaraghavan, M. Indic, B. van den Berg, L. Movileanu, Cation selectivity is a conserved feature in the OccD subfamily of *Pseudomonas aeruginosa*, Biochim. Biophys. Acta -Biomembr. 1818 (2012) 2908–2916.
[71] B.R. Cheneke, B. van den Berg, L. Movileanu, Analysis of gating transitions among the three major open states of the OpdK channel, Biochemistry 50 (2011) 4987–4997.
[72] B.R. Cheneke, M. Indic, B. van den Berg, L. Movileanu, An outer membrane protein undergoes enthalpy- and entropy-driven transitions, Biochemistry 51 (2012) 5348–5358.
[73] J. Liu, E. Eren, J. Vijayaraghavan, B.R. Cheneke, M. Indic, B. van den Berg, L. Movileanu, OccK channels from *Pseudomonas aeruginosa* exhibit diverse single-channel electrical signatures, but conserved anion selectivity, Biochemistry 51 (2012) 2319–2330.
[74] J.D. Faraldo-Gomez, G.R. Smith, M.S. Sansom, Setting up and optimization of membrane protein simulations, Eur. Biophys. J. 31 (2002) 217–227.
[75] J.D. Faraldo-Gomez, G.R. Smith, M.S. Sansom, Molecular dynamics simulations of the bacterial outer membrane protein FhuA: a comparative study of the ferrichrome-free and bound states, Biophys. J. 85 (2003) 1406–1420.
[76] P.J. Bond, J.P. Derrick, M.S. Sansom, Membrane simulations of OpcA: gating in the loops? Biophys. J. 92 (2007) L23–L25.
[77] B. Luan, M. Caffrey, A. Aksimentiev, Structure refinement of the OpcA adhesin using molecular dynamics, Biophys. J. 93 (2007) 3058–3069.
[78] B. Luan, R. Carr, M. Caffrey, A. Aksimentiev, The effect of calcium on the conformation of cobalamin transporter BtuB, Proteins 78 (2010) 1153–1162.
[79] T. Husslein, D.M. Newns, P.C. Pattnaik, Q.F. Zhong, P.B. Moore, M.L. Klein, Constant pressure and temperature molecular-dynamics simulation of the hydrated diphytanolphosphatidylcholine lipid bilayer, J. Chem. Phys. 109 (1998) 2826–2832.
[80] W. Dowhan, M. Bogdanov, Functional role of lipids in membranes, in: D.E. Vance, J.E. Vance (Eds.), Biochemistry of Lipids, Lipoproteins and MembranesElsevier Science B.V., Amsterdam, The Netherlands, 2002, pp. 1–35.